J|A|C|S ARTICLES

Published on Web 07/12/2010

Origin of Pressure Effects on Regioselectivity and Enantioselectivity in the Rhodium-Catalyzed Hydroformylation of Styrene with (*S*,*S*,*S*)-BisDiazaphos

Avery L. Watkins and Clark R. Landis*

Department of Chemistry, University of Wisconsin-Madison, 1101 University Avenue, Madison, Wisconsin 53706

Received November 19, 2009; E-mail: landis@wisc.edu

Abstract: Gas pressure influences the regioselectivity and enantioselectivity of aryl alkene hydroformylation as catalyzed by rhodium complexes of the BisDiazaphos ligand. Deuterioformylation of styrene at 80 °C results in extensive deuterium incorporation into the terminal position of the recovered styrene. This result establishes that rhodium hydride addition to form a branched alkyl rhodium occurs reversibly. The independent effect of carbon monoxide and hydrogen partial pressures on regioselectivity and enantioselectivity were measured. From 40 to 120 psi, both regioisomer (b:l) and enantiomer (*R*:*S*) ratios are proportional to the carbon monoxide partial pressure but approximately independent of the hydrogen pressure. The absolute rate for linear aldehyde formation was found to be inhibited by carbon monoxide pressure, whereas the rate for branched aldehyde formation is independent of CO pressure up to 80 psi; above 80 psi one observes the onset of inhibition. The carbon monoxide dependence of the rate and enantioselectivity for branched aldehyde indicates that the rate of production of (*S*)-2-phenyl propanal is inhibited by CO pressure, while the formation rate of the major enantiomer, (*R*)-2-phenyl propanal, is approximately independent of CO pressure. Hydroformylation of α-deuteriostyrene at 80 °C followed by conversion to (*S*)-2-benzyl-4-nitrobutanal reveals that 83% of the 2-phenylpropanal resulted from rhodium hydride addition to the *re* face of styrene, and 83% of the 3-phenylpropanal resulted from rhodium hydride addition to the *si* face of styrene. On the basis of these results, kinetic and steric/electronic models for the determination of regioselectivity and enantioselectivity are proposed.

Introduction

Asymmetric hydroformylation (AHF) is an efficient, low-cost route to chiral aldehydes from prochiral alkenes.[1] Because aldehydes are such versatile synthetic intermediates, AHF could be a key transformation in the production of chiral pharmaceuticals and agrochemicals.[2] Aryl alkenes are attractive substrates for AHF primarily because oxidation of the branched aldehyde to the corresponding 2-arylpropionic acid yields pharmacologically active, anti-inflammatory analgesics such as ibuprofen, ketoprofen, and naproxen.

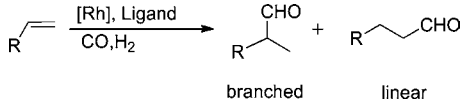

However, practical application of AHF faces several challenges. Production of a single branched aldehyde with high enantiomeric purity requires precise control of chemo-, enantio-, and regioselectivity. Large-scale application requires high catalyst rates and large turnover numbers, particularly when expensive metals and chiral ligands are used. In view of these challenges, only a small number of catalyst systems capable of achieving useful productivity of a single enantiomer with >90% ee have been reported for rhodium-catalyzed AHF.[3] Among the successful ligands reported, BINAPHOS and (*S*,*S*,*S*)-BisDiazaphos (**1**) ligands have been demonstrated to exhibit selectivity for structurally diverse alkenes.[4,5] Using **1** and rhodium catalyst precursors, we have found that AHF of terminal aryl alkenes exhibits complex behavior as a function of the gas partial pressures.[6] Increased CO pressure yields higher regioselectivity and enantioselectivity but suppresses the rate. In contrast, changes in H_2 pressure have little influence. We seek a better understanding of the origin of regioselectivity and enantioselectivity in AHF.

(1) For recent reviews of AHF, see: (a) Agbossou, F.; Carpentier, J.-F.; Mortreux, A. *Chem. Rev.* **1995**, *95*, 2485–2506. (b) Claver, C.; van Leeuwen, P. W. N. M. *Rhodium Catalyzed Hydroformylation*; Kluwer Academic Publishers: Dordrecht, 2000. (c) Breit, B.; Wolfgang, S. *Synthesis* **2001**, *1*, 1–36. (d) Dieguez, M.; Pamies, O.; Claver, C. *Tetrahedron: Asymmetry* **2004**, *15*, 2113–2122. (e) Dieguez, M.; Pamies, O.; Claver, C. *Top. Organomet. Chem.* **2006**, 35–64.

(2) Botteghi, C.; Paganelli, S.; Marchetti, M. *Chirality* **1991**, *3*, 355–369.

(3) For successful ligands for AHF, see: (a) Babin, J. E.; Whiteker, G. T. World Patent WO 9393839, 1993. (b) Sakai, N.; Mano, S.; Nozaki, K.; Takaya, H. *J. Am. Chem. Soc.* **1993**, *115*, 7033–7034. (c) Dieguez, M.; Pamies, O.; Ruiz, A.; Claver, C. *New J. Chem.* **2002**, *26*, 827–833. (d) Cobley, C. J.; Gardner, K.; Klosin, J.; Praquin, C.; Hill, C.; Whiteker, G. T.; Zanotti-Gerosa, A.; Petersen, J. L.; Abboud, K. A. *J. Org. Chem.* **2004**, *69*, 4031–4040. (e) Cobley, C. J.; Klosin, J.; Qin, C.; Whiteker, G. T. *Org. Lett.* **2004**, *6*, 3277–3280. (f) Clark, T. P.; Landis, C. R.; Freed, S. L.; Klosin, J.; Abboud, K. A. *J. Am. Chem. Soc.* **2005**, *127*, 5040–5042. (g) Yan, Y. J.; Zhang, X. M. *J. Am. Chem. Soc.* **2006**, *128*, 7198–7202. (h) Yan, Y. J.; Zhang, X. M. *J. Am. Chem. Soc.* **2006**, *128*, 7198–7202. (i) Axtell, A. T.; Klosin, J.; Abboud, K. A. *Organometallics* **2006**, *25*, 5003–5009.

10.1021/ja909619a

Scheme 1. General Mechanism for Rhodium-Catalyzed Hydroformylation

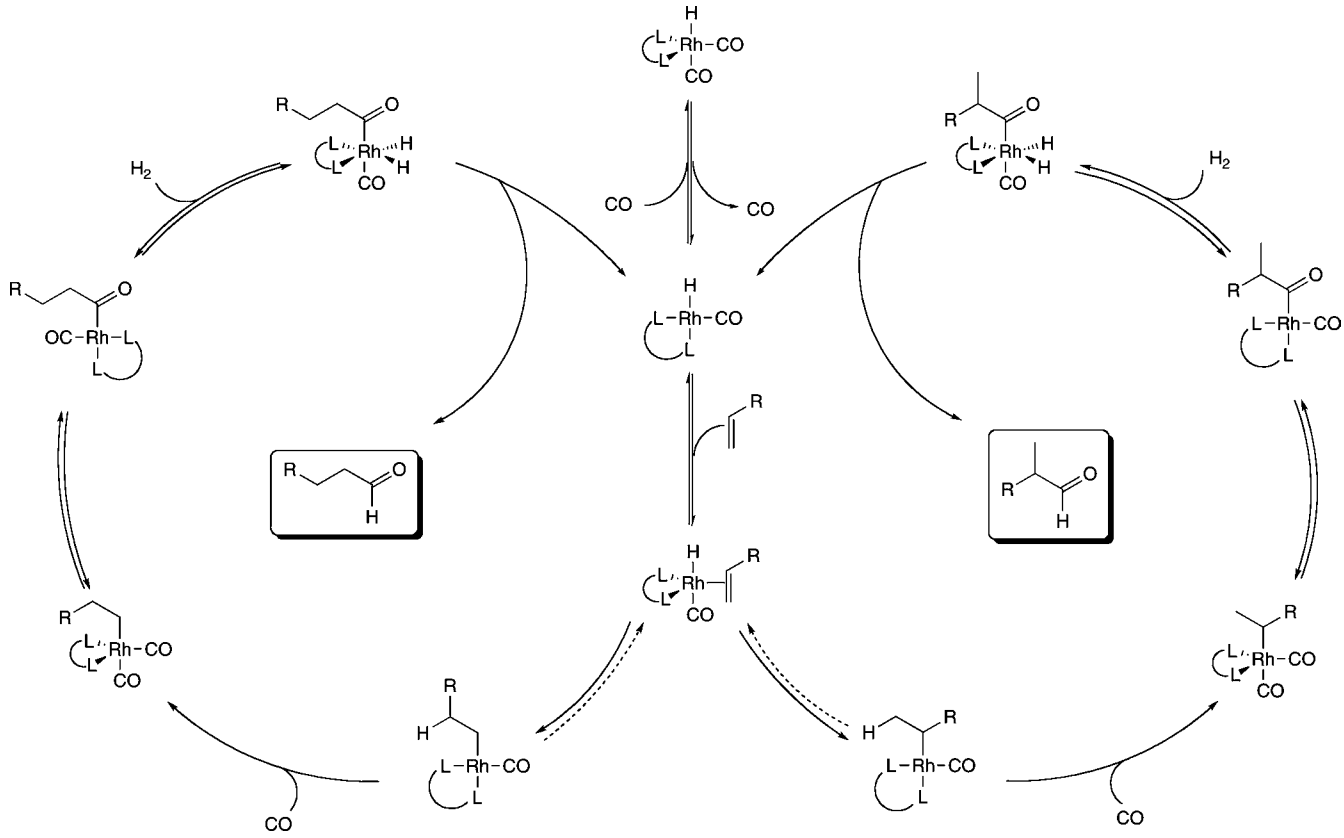

In this contribution, we present the methods, results, and interpretations of mechanistic investigations of styrene hydroformylation using Rh(BisDiazaphos) catalysts. First, we report investigations of AHF using D_2 and CO; these studies probe the reversibility of Rh-D addition to styrene. This is followed by kinetic studies of the effect of CO and H_2 pressures on rates of formation of the achiral linear isomer and both branched enantiomers. Data presentation concludes with isotopic labeling experiments that probe the extent to which the linear product results from reaction at the *re* and *si* faces of styrene. These data are interpreted according to a simple kinetic model that accommodates all the known data and constitutes a robust model for the origins of selectivity and gas pressure effects in AHF of styrene as catalyzed by rhodium complexes of **1**.

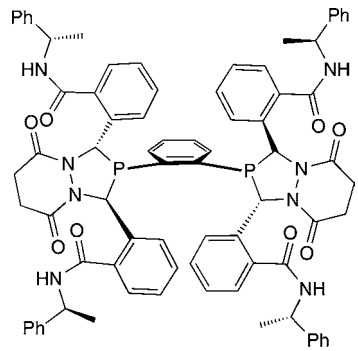

(*S,S,S*)-BisDiazaphos (1)

Background

According to the generally accepted mechanism for hydroformylation, first proposed by Heck and Breslow[7] (Scheme 1), the product regio- and stereoselectivity may be set at one of four stages: (1) irreversible alkene coordination to rhodium, (2) reversible alkene coordination followed by irreversible rhodium hydride addition, (3) reversible rhodium alkyl formation followed by irreversible alkyl migration to CO to form a rhodium acyl complex, or (4) reversible rhodium acyl formation followed by irreversible rhodium acyl hydrogenolysis.

For rhodium-based catalyst systems, the regiochemistry of the aldehydes commonly is thought to be set by largely irreversible hydride addition to coordinated alkene.[8,9] The structure of the five-coordinate π-olefin complex is proposed

(4) (a) Sakai, N.; Nozaki, K.; Takaya, H. *J. Chem. Soc. Chem. Comm.* **1994**, 395–396. (b) Nanno, T.; Sakai, N.; Nozaki, K.; Takaya, H. *Tetrahedron: Asymmetry* **1995**, *6*, 57. (c) Nozaki, K.; Li, W.; Horiuchi, T.; Takaya, H. *Tetrahedron Lett.* **1997**, *38*, 4611–4614. (d) Horiuchi, T.; Ohta, T.; Shirakawa, E.; Nozaki, K.; Takaya, H. *Tetrahedron* **1997**, *53*, 7795–7804. (e) Nozaki, K.; Sakai, N.; Nanno, T.; Higashijima, T.; Mano, S.; Horiuchi, T.; Takaya, H. *J. Am. Chem. Soc.* **1997**, *119*, 4413–4423. (f) Nozaki, K.; Takaya, H.; Hiyama, T. *Top. Catal.* **1997**, *4*, 175–185. (g) Nozaki, K.; Matsuo, T.; Shibahara, F.; Hiyama, T. *Adv.Synth. Catal.* **2001**, *343*, 61–63. (h) Aghmiz, A.; Masdeu-Bulto, A. M.; Claver, C.; Sinou, D. *J. Mol. Catal.* **2002**, *184*, 111–119.

(5) Clark, T. P.; Landis, C. R.; Freed, S. L.; Klosin, J.; Abboud, K. A. *J. Am. Chem. Soc.* **2005**, *127*, 5040–5042.

(6) Watkins, A. L.; Hashiguchi, B. G.; Landis, C. R. *Org. Lett.* **2008**, *10*, 4553–4556.

(7) Heck, R. F.; Breslow, D. S. *J. Am. Chem. Soc.* **1961**, *83*, 4023–4027.

(8) (a) Lazzaroni, R.; Uccello-Barretta, G.; Benetti, M. *Organometallics* **1989**, *8*, 2323–2327. (b) Lazzaroni, R.; Settambolo, R.; Uccello-Barretta, G. *Organometallics* **1995**, *14*, 4644–4650. (c) Casey, C. P.; Petrovich, L. M. *J. Am. Chem. Soc.* **1995**, *117*, 6007–6014. (d) Horiuchi, T.; Shirakawa, E.; Nozaki, K.; Takaya, H. *Organometallics* **1997**, *16*, 2981–2986.

(9) van Leeuwen has reported an example of reversible hydride addition in the hydroformylation of 1-hexene. See: van der Slot, S. C.; Duran, J.; Luten, J.; Kamer, P. C. J.; van Leeuwen, P. W. N. M. *Organometallics* **2002**, *21*, 3873–3833.

to play a crucial role in controlling the regioselectivity of the reaction.[10] However, this π-olefin complex has not been observed directly. Brown and Kent[11] have shown that the PPh_3-modified $L_2Rh(CO)_2H$ complex exists as a mixture of two rapidly equilibration trigonal bipyramidal isomers in a diequatorial (ee) to equatorial-apical (ea) isomer ratio of 85:15. Studies on electronically modified bisphosphine ligands have demonstrated similar dynamic equilibria between ee and ea.[12] Casey and Whiteker[13] developed the concept of the natural bite angle as means of characterizing diphosphine ligands on the basis of molecular mechanics calculations. The Casey group reported that the regioselectivity of the rhodium-catalyzed hydroformylation of 1-alkenes was dramatically affected by the bite angle of bidentate bisphosphine ligands.[14] The correlation between regioselectivity and ligand natural bite angle was rationalized on the basis of a change in the ratio of ee and ae isomers as a function of ligand bite angle. However, subsequent work by Van Leeuween suggests that, despite the correlation between regioselectivity and natural bite angle, the chelation mode of the diphosphine ligand is not the key parameter controlling the regioselectivity.[15]

Reaction conditions dictate which step fixes the regioselectivity of rhodium-catalyzed aryl alkene hydroformylation.[16] For styrene hydroformylation with unmodified rhodium catalysts, rhodium hydride addition strongly favors production of the branched isomer and is irreversible at low temperature reaction conditions (25−80 °C, 10−20 atm syngas). However, at higher temperatures (90−120 °C), rhodium hydride addition can become reversible. Under these conditions regioselectivity is controlled as combination of the alkene insertion step and subsequent steps such as CO binding and acyl formation.

Compared with achiral catalyst systems, the mechanistic details of rhodium-catalyzed asymmetric hydroformylation reactions are poorly understood. By analogy to achiral systems, the regiochemistry and stereochemistry of AHF should be set by the hydride addition step. On this basis, the origin of enantioselectivity in asymmetric hydroformylation has been discussed with the simple model proposed by Pino and Consiglo.[17] However, Nozaki and co-workers found that in the AHF of styrene with BINAPHOS, the hydride addition becomes reversible when the syngas pressure is reduced from 10 to 1 atm.[18] Concomitant with the onset of reversibility was a modest decrease in both regioselectivity and enantioselectivity (from 9:1 b:l to 5:1 and from 94% to 89% ee). We also observe strong gas pressure effects on the regio- and stereochemistry of aryl alkene AHF using Rh(BisDiazaphos) catalysts (vide supra). If

Scheme 2. Asymmetric Hydroformylation of Styrene under Standard Conditions

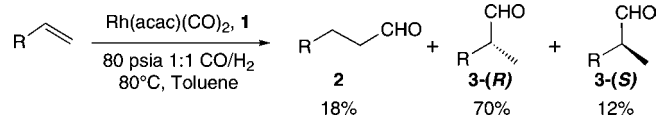

alkyl rhodium formation is reversible, the regio- and enantioselectivity must also be controlled, at least in part, by a step (or steps) occurring later in the catalytic cycle. Casey et al.[19] found that the nature of the selectivity-determining steps for Pt-catalyzed hydroformylation of styrene changed with temperature and gas pressures. On the basis of deuterioformylation studies, they showed that enantioselectivity was determined in the hydride addition step at 40 °C but at 100 °C was controlled in latter stages of the catalytic cycle. Understanding the effect of CO and H_2 pressures on the selectivity is critical to determining the origin of selectivity in AHF.

Results

Hydroformylation of Styrene at 80 °C. Standard conditions (Scheme 2) for these hydroformylation studies comprise styrene at 2.9 M and Rh-BisDiazaphos catalyst (**1**) at 6.7×10^{-4} M in toluene (1.5 mL total solution volume) at 80 °C with 80 psi syngas (1:1 CO/H_2) performed in a pressure bottle (total volume ca. 50 mL) placed in an oil bath and fitted with a Teflon-coated stir bar. At 90% conversion of styrene, chiral GC analysis showed 3-phenylpropanal (**2**) and 2-phenyl propanal (**3**) [branched:linear (b:l) = 4.5:1, 71% ee 2-phenylpropanal (**3(*R*)**)]. In separate experiments, the regioselectivity and enantioselectivity were observed to remain constant throughout the reactions. These results were in good agreement with earlier studies that were performed on a larger scale.

Deuterioformylation of Styrene. The reversibility of rhodium hydride addition to coordinated styrene was probed with deuterioformylation experiments. If hydride addition were irreversible, deuterium would be incorporated in the product with one deuterium β to the carbonyl group and one in the formyl group (Scheme 3), only. However, reversible hydride addition could yield incorporation of deuterium in multiple sites of both styrene and the aldehyde products. Quenching the reaction at low substrate conversion (<10% conversion) minimizes the possibility of multiple exchanges and the opportunity for deuterium-exchanged styrene to undergo deuterioformylation. Under such conditions one expects the major deuterium-containing products to be the dideuterio-aldehyde products (linear and branched) and deuterium-exchanged styrene; appearance of deuterium in the α-position of styrene indicates reversible formation of the linear Rh-alkyl, whereas reversible formation of the branched alkyl is implicated by observation of deuterium in the β (or terminal) position.

Deuterioformylation of styrene catalyzed by **1** was conducted at 80 psi 1:1 CO/D_2 at 80 °C. After 10 min of reaction time, ^1H NMR analysis showed that 5% of the styrene had been converted to aldehydes with b:l = 4.2 and 69% ee **3(*R*)**. Integration of ^1H and ^2H spectra of the products revealed 100% incorporation of deuterium in the formyl group of the aldehyde products (Scheme 4, **A**−**D**) but only 20% deuterium incorporation β to the carbonyl groups (**B** and **C**). No deuterium was observed at the position α to the carbonyl groups of either aldehyde regioisomer

(10) Casey, C. P.; Whiteker, G. T.; Melville, M. G.; Petrovich, L. M.; Gavney, J. A.; Powell, D. R. *J. Am. Chem. Soc.* **1992**, *114*, 5535–5543.
(11) Brown, J. M.; Kent, A. G. *J. Chem. Soc., Perkin Trans. 2* **1987**, 1597–1607.
(12) Casey, C. P.; Paulsen, E. L.; Beuttenmueller, E. W.; Proft, B. R.; Petrovich, L. M.; Matter, B. A.; Powell, D. R. *J. Am. Chem. Soc.* **1997**, *119*, 11817–11825.
(13) Casey, C. P.; Whiteker, G. T. *Isr. J. Chem.* **1990**, *30*, 299–304.
(14) Casey, C. P.; Whiteker, G. T.; Melville, M. G.; Petrovich, L. M.; Gavney, J. A.; Powell, D. R. *J. Am. Chem. Soc.* **1992**, *114*, 5535–5543.
(15) van der Veen, L. A.; Boele, M. D. K.; Bregman, F. R.; Kamer, P. C. J.; van Leeuwen, P. W. N. M.; Goubitz, K.; Fraanje, J.; Schenk, H.; Bo, C. *J. Am. Chem. Soc.* **1998**, *120*, 11616–11626.
(16) Lazzaroni, R.; Raffaelli, A.; Settambolo, R.; Bertozzi, S.; Vitulli, G. *J. Mol. Catal.* **1989**, *50*, 1–9.
(17) Consiglio, G.; Pino, P. *Top. Curr. Chem.* **1982**, *105*, 77–123.
(18) Nozaki, K.; Matsuo, T.; Shibahara, F.; Hiyama, T. *Organometallics* **2003**, *22*, 594–600.
(19) Casey, C. P.; Martins, S. C.; Fagan, M. A. *J. Am. Chem. Soc.* **2004**, *126*, 5585–5592.

Scheme 3. Products Expected from Deuterioformylation of Styrene

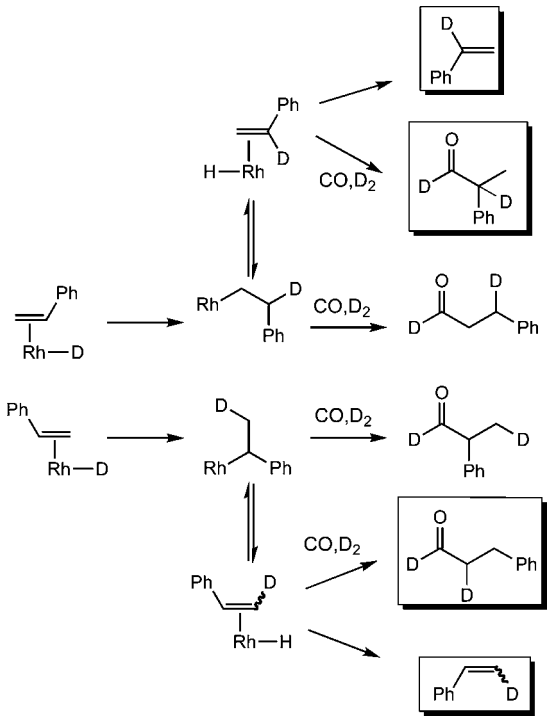

Scheme 4. Product Distribution Observed in the Deuterioformylation of Styrene Performed under Standard Conditions[a]

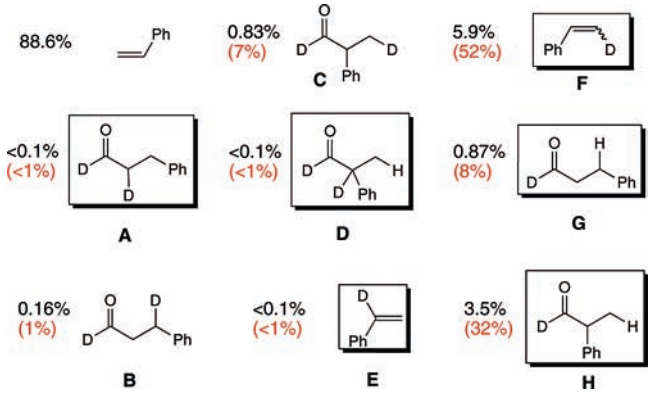

[a] Products outlined by boxes require reversible insertion of styrene into the Rh-D bond. Percentages outside of parentheses indicate product yield based on initial styrene; percentages within indicate fractional yields among transformed styrene molecules.

(**A** and **D**). Of the recovered styrene, 5.9% contained deuterium in the β vinyl positions (**F**). No deuterium was found at the α-vinyl position of the recovered styrene (**E**). Thus, of the approximately 11% of the initial styrene that was transformed, 48% yielded aldehydes and 52% gave β-deuteriostyrene. The gas headspace above the reactor is sufficiently large (50 mL) that the accumulated HD is less than 5% of the H_2 present.

The extensive incorporation of deuterium in the recovered styrene requires reversible formation of the branched rhodium alkyl. Once formed, this deuterated alkyl rhodium complex β-hydride eliminates to give β-deuteriostyrene about 7 times faster than it is converted to aldehyde (51.2% **F** vs 7.2% **C**). Taking labeling statistics (1/3 of reversions of branched rhodium alkyl to styrene leave an isotopic trace) into account and assuming no significant isotope effect, the branched alkyl rhodium complex reverts to styrene approximately 21 times

Scheme 5. Pathways by Which d_1-Aldehydes and β-d_1-Styrene Are Produced

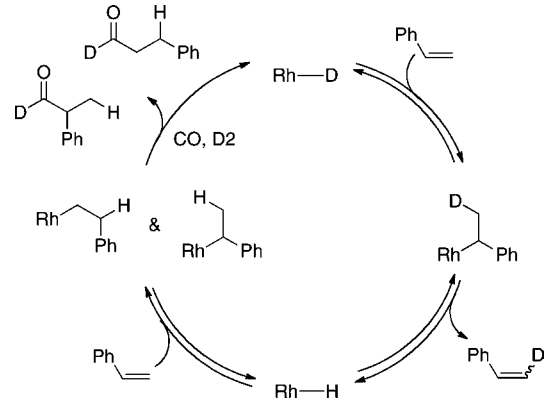

faster than it converts to aldehdye. Much more deuterium shows up in the recovered styrene than in the β-position of the aldehydes (51% **F** compared to 9% (**B** + **C**)), suggesting that when a branched rhodium alkyl reverts to a rhodium alkene hydride, the styrene most frequently dissociates from rhodium. Styrene complexation to rhodium is apparently rapid and reversible as compared to rhodium hydride addition. Because deuterium is not found in the internal α position of the unreacted styrene, linear alkyl rhodium appears much more likely than branched alkyl rhodium to progress to aldehyde without competitive reversion to styrene. However, some caution is required in interpreting this result because the methylene hydrogens of the linear alkyl are diastereotopic and could undergo β-hydride elimination stereospecifically such that deuterium exchange does not result.

Most of the aldehydes formed during deuterioformylation under standard conditions have just one deuterium in the product. Although all linear and branched formyl groups contain deuterium, the β-positions of the aldehyde products are primarily protio (80% (**G** + **H**)). The high level of protium in the β-position of the aldehyde suggests a 4-fold higher steady-state concentration of Rh-H species than Rh-D species. Although acyl hydrogenolysis regenerates rhodium deuterides exclusively, the deuterium is rapidly incorporated into the unreacted styrene by a rapid hydride addition/β-hydride elimination sequence (see Scheme 5).

Hydroformylation Selectivity Varies with CO Pressure. The independent effects of CO and H_2 partial pressure on the regioselectivity and enantioselectivity of styrene hydroformylation as catalyzed by **1** at 80 °C was investigated. One set of experiments used 40 psi H_2 pressure while varying CO pressure systematically from 15 to 200 psi.

As shown in Figure 1, both the branched:linear aldehyde ratio (b:l) and the enantiomeric ratio (*R*:*S*) show a strong dependence on the CO pressure. The experimental data for b:l and *R*:*S* ratios roughly conform to a phenomenological rate expression of the type shown in eq 1.

$$\text{rate ratio} = \frac{A[\text{CO}]}{B + C[\text{CO}]} \qquad (1)$$

Competitive trapping by CO results in a transition from apparent first order dependency in the low CO pressure regime to independence in the high CO pressure regime. Many scenarios could give rise to his kinetic behavior. However, the conclusion (from analysis of deuterioformylation results) that some reversibility accompanies branched alkyl formation immediately

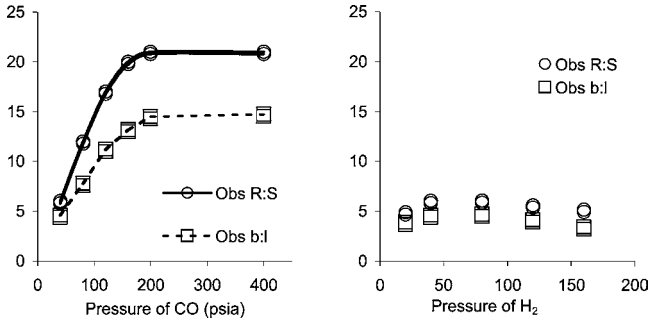

Figure 1. Graphs depicting the influence of CO and H_2 pressure on the enantiomeric ratio (*R*:*S* = [**3(R)**]/[**3(S)**]) and branched:linear aldehyde ratio (b:l = [**3**]/[**2**]) for styrene hydroformylation catalyzed by **1** at 80 °C in toluene. Smoothed trend lines are visual aids only.

suggests a role of CO in the competition between β-hydride elimination from a branched alkyl rhodium species and conversion to aldehyde product. For example, coordination of CO to a branched alkyl rhodium species may promote acyl formation and, hence, production of branched aldehyde. Because increased CO pressure influences the enantiomeric ratio also, it appears that the reaction manifold that leads to **3(*R*)** is most affected. Thus, raising the CO pressure could promote formation of **3(*R*)** over both **2** and **3(*S*)**, which would simultaneously increase reaction regioselectivity and enantioselectivity.

Hydroformylation Selectivity Is Independent of H_2 Pressure. To independently measure the effect of H_2 partial pressure on regio- and enantioselectivity, the catalytic hydroformylation of styrene in the presence of Rh-BisDiazaphos (**1**) at 80 °C was performed under different H_2 pressures. The CO pressure was held at constant 40 psi, and the H_2 partial pressure was varied from 15 to 160 psi. As shown in Figure 1, neither the regioselectivity (b:l) nor enantioselectivity (*R*:*S*) varied appreciably as the H_2 pressure was changed. Therefore, both the regiochemistry and stereochemistry of the reaction are likely set prior to acyl hydrogenolysis.

Rates of Product Formation and Deuterium Exchange Vary with CO Pressure. The data provided so far address the relative but not absolute rates of **2**, **3(*R*)**, and **3(*S*)** formation. Absolute rates were probed by deuterioformylation experiments in which the D_2 pressure is held constant at 40 psi, and the CO pressure was varied systematically from 40 to 160 psi. Comparison with experiments performed under H_2 revealed no measurable deuterium isotope effect on either the b:l or *R*:*S* ratios. Simulation of the initial deuterioformylation rates at <10% conversion according to a simple kinetic model (Scheme 6) using the kinetic modeling software package COPASI[20] leads to an excellent fit to experimental data for the appearance of dideuterio and monodeuterio isotopologues of linear and branched aldehydes and for monodeuterio styrene using just three unique, phenomenological rate constants (all kinetic isotope effects are assumed to be small). Because the CO and D_2 pressures are constant during each experiment, each step in the kinetic model has a rate given by the product of the styrene concentration, catalyst concentration, and rate constant. For example, the following rate equation describes deuterium incorporation into styrene, the last step in the kinetic model: $\delta[d_1\text{-styrene}]/\delta t = k_{exchange}$[Rh-D][styrene]. Kinetic modeling is required because the distribution of catalyst between Rh-H and

(20) Hoops, S.; Sahle, S.; Gauges, R.; Lee, C.; Pahle, J.; Simus, N.; Singhal, M.; Xu, L.; Mendes, P.; Kummer, U. *Bioinformatics* **2006**, *22*, 3067–3074.

Scheme 6. Kinetic Scheme Used To Extract Phenomenological Rate Constants (k_{linear}, $k_{branched}$, $k_{exchange}$) by Simulation of Product Concentrations Observed for Deuterioformylation of Styrene As Catalyzed by $Rh(acac)(CO)_2$ in the Presence of **1** at Small Conversions

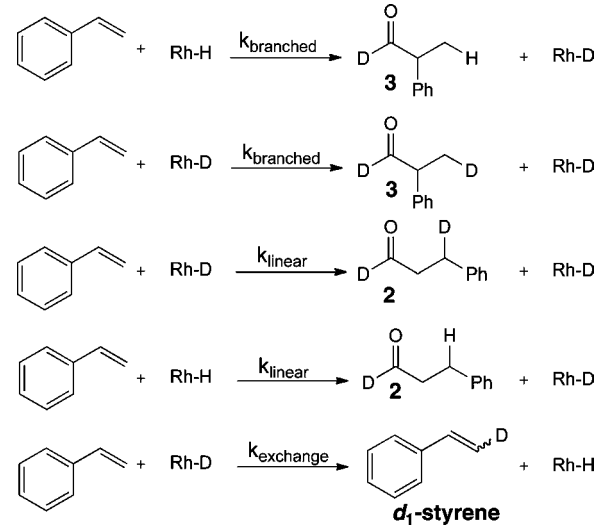

Rh-D changes during the initial rate period as H is scrambled from styrene to the catalyst under D_2.

Data for the effect of CO pressure on the observed rate constants for formation of **2** and **3** and d_1-styrene are shown in Figure 2. The rate constant for H/D exchange is greater than the respective rates for both **2** and **3**, even at high CO pressure. The rates of linear aldehyde **2** formation and H/D exchange into unlabeled styrene are inhibited by increasing CO pressure.

Inhibition by CO plausibly results from the need to dissociate CO from the catalyst resting state, $HRh(CO)_2L$, in order to generate HRh(CO)L, which is capable of reacting with styrene.

The effect of P_{CO} on the rate of branched aldehyde formation is more complex. In the low pressure region, the rate is unaffected by increasing P_{CO}. However, at higher pressures, the rate appears to be slightly inhibited by increasing P_{CO}.

Separation of the rates for branched aldehyde formation into rates for each enantiomer (see Figure 2) provides further insight into the influence of pressure on regioselectivity and enantioselectivity. The phenomenological rate constant $k_{branched}$ comprises the sum of the rate constants, $k_{branched(R)} + k_{branched(S)}$, for the two enantiomeric products. As shown in Figure 2, plots of apparent rate constants as a function of CO pressure indicate that the rate for minor enantiomer **3(*S*)** is inhibited by CO pressure, whereas formation of **3(*R*)** is independent of CO, perhaps exhibiting the onset of inhibition at higher pressure.

Hydroformylation Rates Exhibit Linear Dependence on Catalyst and Alkene Concentration. The effect of catalyst and alkene concentrations on hydroformylation rates is depicted in Figure 3. A plot of the initial rate of aldehyde formation versus catalyst concentrations (0.2 to 2 mM) indicates a first-order dependence on catalyst concentration. The reaction order with respect to alkene was determined by monitoring the entire reaction time course using in situ infrared spectroscopy. As shown in Figure 3, the formation of aldehyde exhibits a well-behaved first-order dependence on alkene concentration.

Hydroformylation of α-Deuteriostyrene Reveals the Regioselectivity for Different Styrene Enantiofaces. Under the hydroformylation conditions examined thus far, rhodium hydride adds preferentially to the *re* face of complexed styrene to form

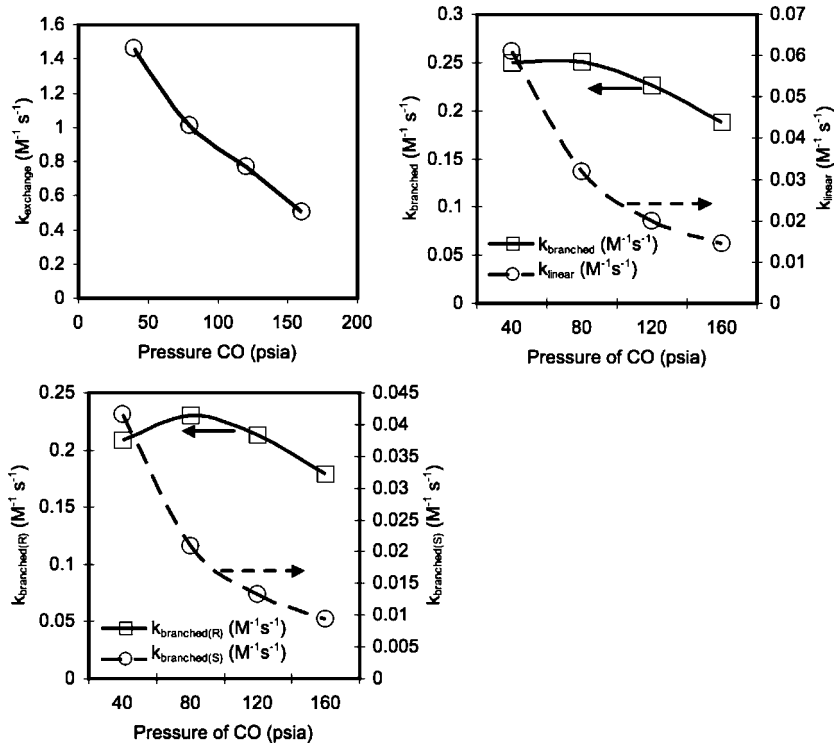

Figure 2. Graphs depicting the influence of CO pressure on the observed rate constants for formation of d_1-styrene ($k_{exchange}$, upper left plot), 3-phenylpropanal and 2-phenylpropanal (k_{linear} and $k_{branched}$, upper right), and the partitioning of the branched rate constant into (*R*)-2-phenylpropanal and (*S*)-2-phenylpropanal components ($k_{branched(R)}$ and $k_{branched(S)}$, lower left). All reactions performed at 80 °C, $[styrene]_0 = 2.9$ M, $[\mathbf{1}] = 6.7 \times 10^{-4}$ M, $P_{H_2} = 40$ psi. Smoothed lines serve as guides only.

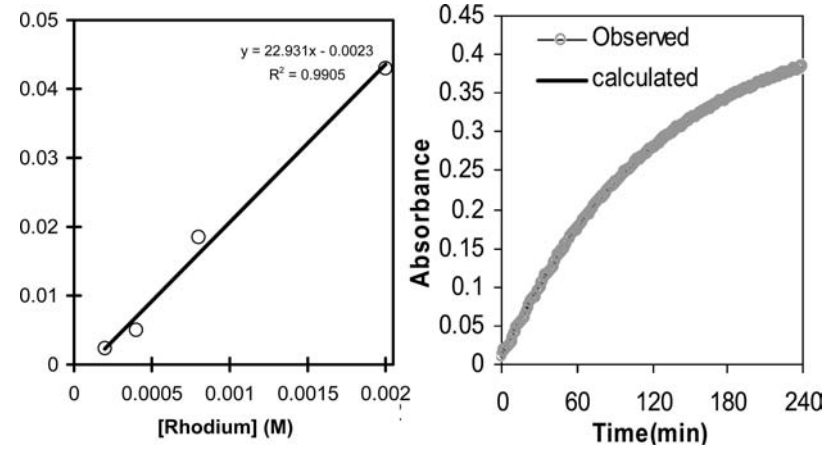

Figure 3. Effects of catalyst (left) and styrene concentrations (right) on reaction rate for reactions performed at 80 °C, 80 psi syngas, $[styrene]_0 = 2.9$ M. The left plot shows initial rates measured at varying concentrations of catalyst. The right-hand plot represents the IR absorbance due to aldehyde products as a function of time as monitored at 1725 cm^{-1} and the line computed for a simple first-order dependence on styrene.

the branched rhodium alkyl that ultimately produces the major aldehyde product **3(*R*)**. Although the other enantiomer, **3(*S*)**, arises from binding the *si* face of styrene to the catalyst, it is not clear if the linear isomer originates primarily from the *si* or *re* face of the styrene-Rh adduct. To examine the stereochemistry of 3-phenylpropanal formation, the hydroformylation of α-deuteriostyrene was carried out and the stereochemistry of the deuterated 3-phenylpropanal was determined (Scheme 7). We note that an alternative strategy, the hydroformylation of *β*-deuteriostyrene, was precluded by the rapid exchange of H and D in the *β*-position during the hydroformylation (vide supra).

Hydroformylation of α-deuteriostyrene in the presence of **1** at 80 °C under 80 psi 1:1 CO/H_2 for 6 h showed that 99% of the styrene had been converted to **2** and **3** with b:l = 4.3 and 63% ee **3(*R*)**. The stereochemistry of **2** was determined by conversion to the diastereomeric (2)-benzyl-4-nitrobutanal **6**, using the enantioselective organocatalytic Michael addition protocol developed by Gellman and co-workers.[21] The ratio of diastereomers **6a** and **6b** was determined by ^{2}H NMR integrations of the diastereotopic benzylic methylene protons (PhH**D**C) resonances, which appear at 3.17 and 2.8 ppm, respectively. The 5:1 ratio of these resonances gives 63% de, which is similar to 63% ee. Molecular mechanics modeling of conformational distributions and experimental ^{1}H NMR NOEs establish that

(21) Chi, Y.; Guo, L.; Kopf, N. A.; Gellman, S. H. *J. Am. Chem. Soc.* **2008**, *130*, 5608–5609.

Scheme 7. Determination of Linear Product (3-Phenylpropanal) Stereochemistry Obtained by Hydroformylation of α-d_1-Styrene

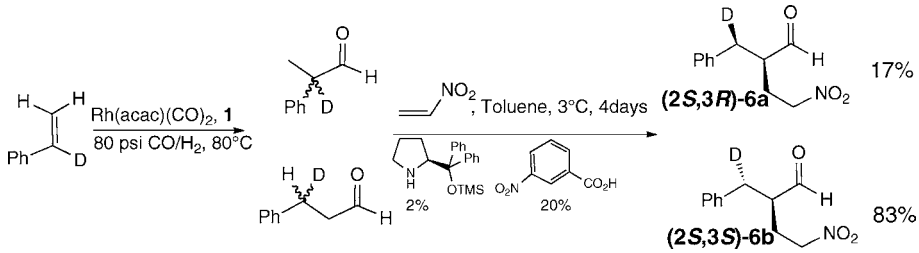

Scheme 8. Stereochemical Outcome of the Rhodium-Catalyzed Hydroformylation of α-d_1-Styrene in the Presence of **1**

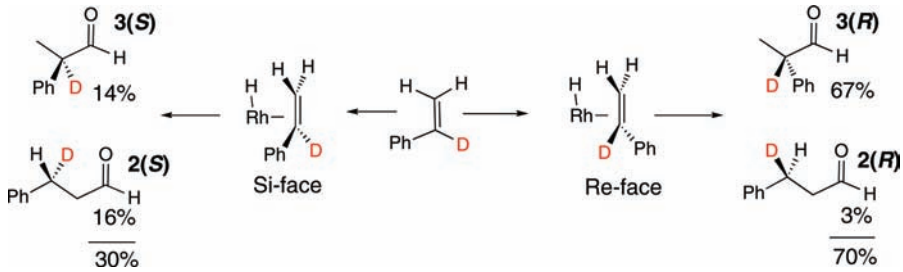

Scheme 9. Proposed Kinetic Model for Determination of Regioselectivity in AHF of Styrene

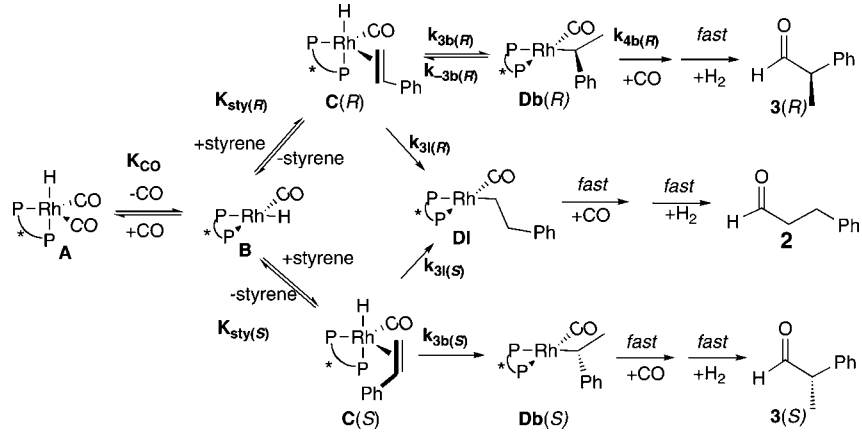

(2*S*,3*S*)-**6b** forms in excess. Thus, **2** is generated primarily from hydride addition to the *si* face of coordinated styrene.[22]

The stereochemistry of aldehyde formation under the conditions used for the hydroformylation of α-deuteriostyrene is summarized in Scheme 8. The branched isomer, 2-phenylpropanal, constitutes 81% of the aldehydes; 83% of the branched aldehyde is formed by rhodium hydride addition to the *re* face of styrene. In contrast, 3-phenylpropanal constitutes 19% of the aldehydes, and 84% of it is formed by rhodium hydride addition to the *si* face of styrene. Overall, 70% of the aldehyde products result from rhodium hydride addition to the *re* face of styrene. While rhodium hydride addition to the *re* face of styrene exhibits excellent selectivity toward branched aldehydes (22:1 b:l), rhodium hydride addition to the *si* face of styrene is unselective, resulting in neapear aldehydes. Casey and co-workers reported a similar selectivity trend for the platinum catalyzed AHF of styrene.[19]

Discussion

Proposed Kinetic Model for Hydroformylation. On the basis of the experimental kinetic and isotopic labeling data, we propose the kinetic model for enantioselective hydroformylation shown in Scheme 9. This model differs from the mechanism shown in Scheme 1 by the addition of diastereomeric pathways that produce enantiomers **3(*R*)** and **3(*S*)**. Starting from 18 e^- complex **A**, loss of CO generates catalytically active **B**. Coordination of styrene to **B** yields the diasteremeric alkene complexes **C(*S*)** and **C(*R*)**. From alkene complex **C(*S*)**, in which the alkene is coordinated at its *si* face, rhodium hydride can then add to the coordinated styrene to give a linear alkyl rhodium complex **Dl** or a branched alkyl rhodium complex **D(*S*)**. These rhodium alkyls are formed irreversibly and, hence, are committed to forming **2** and **3(*S*)**. Rhodium hydride addition from **C(*R*)**, in which styrene is coordinated at the *re* face, can lead to either the linear rhodium alkyl **Dl** or the branched rhodium alkyl **D(*R*)**. Whereas the linear alkyl **Dl** is formed irreversibly, branched **D(*R*)** undergoes reversion to styrene via β-hydride elimination at a rate that is competitive, depending on the CO pressure, with conversion to aldehyde. Thus, for the reaction manifolds leading to **2** and **3(*S*)**, rhodium hydride addition fixes the selectivity and limits the turnover frequency. Qualitatively, inhibition of the flux by CO along these manifolds results from shifting of the equilibrium **A**·**B** + CO toward **A**. For **3(*R*)**, the turnover frequency is determined by the product of the frequency of hydride addition to give **Dl(*R*)** multiplied by the fraction of

(22) The absolute stereochemistry at C-2 has been previously assigned as the *S*-enantiomer (see ref 21).

additions that are trapped to give **3(*R*)**; this fraction is proportional to CO pressure. Qualitatively, the rate of formation of **3(*R*)** is independent of CO pressure due to a cancellation of the inhibitory term (due to shifting of the equilibrium **A**·**B** + CO) by the trapping efficiency term (which increases with CO pressure until it reaches near unity).

A full rate expression for the proposed kinetic model can be derived straightforwardly by application of the steady state approximation on all rhodium-containing species. Because of the many steps and intermediates, it is useful to simplify the treatment with some reasonable approximations. The rate expressions of eqs 2−5 result from the assumptions that (1) the equilibrium between **A** and **B** is rapid as compared to hydride addition, (2) equilibration of **B** with **C**(*R*) and **C**(*S*) is rapid, (3) trapping of the alkyl intermediates **Dl** and **Db(*S*)**, but not **Db(*R*)**, is rapid at all CO pressures, (4) the concentration of **Db(*R*)** is described well by the steady-state approximation, and (5) nearly all of the catalyst pools in the form of **A**, i.e., $[Rh_{TOT}] \approx [\mathbf{A}]$. With these assumptions, the rate expressions for **2**, **3(*R*)**, and **3(*S*)** adopt the forms shown in eqs 2−4.

$$\text{rate}^{\mathbf{2}} = \frac{\text{d}[\mathbf{2}]}{\text{d}t} = \frac{K_{CO}(K_{Sty(R)}k_{\mathbf{3l(R)}} + K_{Sty(S)}k_{\mathbf{3l(S)}})[Rh_{TOT}][\text{styrene}]}{P_{CO}} \tag{2}$$

$$\text{rate}^{\mathbf{3(S)}} = \frac{\text{d}[\mathbf{3(S)}]}{\text{d}t} = \frac{K_{CO}K_{Sty(S)}k_{\mathbf{3b(S)}}[Rh_{TOT}][\text{styrene}]}{P_{CO}} \tag{3}$$

$$\text{rate}^{\mathbf{3(R)}} = \frac{\text{d}[\mathbf{3(R)}]}{\text{d}t} = \frac{K_{CO}K_{Sty(R)}k_{\mathbf{3b(R)}}k_{\mathbf{4b(R)}}[Rh_{TOT}][\text{styrene}]}{k_{-\mathbf{3b(R)}} + k_{\mathbf{4b(R)}}P_{CO}} \tag{4}$$

$$\text{rate}^{\text{D-styrene}} = \frac{\text{d}[\text{D-styrene}]}{\text{d}t} = \frac{{}^1/_3K_{CO}K_{Sty(R)}k_{\mathbf{3b(R)}}k_{-\mathbf{3b(R)}}[Rh_{TOT}][\text{styrene}]}{P_{CO}(k_{-\mathbf{3b(R)}} + k_{\mathbf{4b(R)}}P_{CO})} \tag{5}$$

These rate expressions agree with the kinetic data. For example, the net rates of formation of **2** and **3(*S*)** exhibit inhibition by CO due to the CO-dependent initial pre-equilibrium between **A**, CO, and **B**. For **3(*R*)**, trapping of **Db(*R*)** is inefficient at low CO pressure ($k_{-\mathbf{3b(R)}} > k_{\mathbf{4b(R)}}[CO]$); this causes the rate of its formation to be approximately independent of CO. Upon raising the CO pressure, trapping of **Db(*R*)** by CO becomes competitive with β-hydride elimination ($k_{\mathbf{4b(R)}}[CO] \approx k_{-\mathbf{3b(R)}}$) and the rate of **3(*R*)** formation should be inhibited by CO. In the limit of high CO pressure, the rates of formation of all products are inhibited by CO and the regioselectivity and enantioselectivity reach limiting values. The data are insufficient to uniquely determine all nine constants in eqs 2−5. Therefore, the data were fit to the simpler expressions of eqs 6−9

Global fitting of the four phenomenological rate constants (k_{linear}, $k_{branched(R)}$, $k_{branched(S)}$, and $k_{exchange}$), which were measured over the CO pressure range of 40−160 psi, and the observed **3**:**2** and **3(*R*)**:**3(*S*)** ratios, which were measured over the CO pressure range of 40−400 psi, yield the results shown in eqs 6−9 and Figure 4. For $k_{branched(R)}$ and $k_{exchange}$, both one and two parameter fits were performed. Effectively the two parameter fit tests the sensitivity to a two-term denominator ($a + bP_{CO}$) versus a single term. For the exchange rate

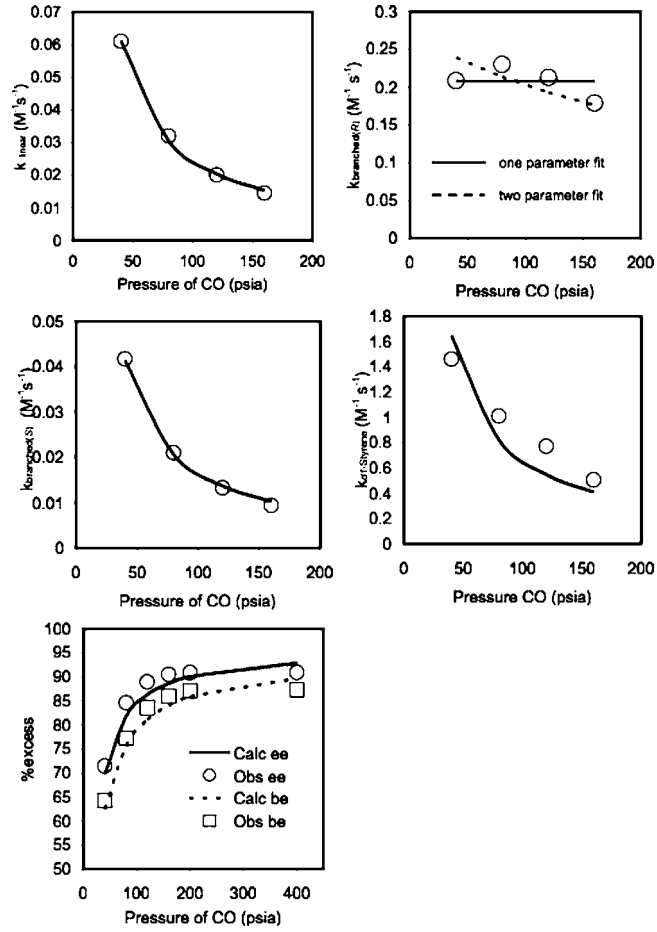

Figure 4. Plots illustrating phenomenological rate constants k_{linear}(upper left), $k_{branched(R)}$(upper middle), $k_{branched(S)}$ (middle left), $k_{exchange} = k_{d_1\text{-styrene}}$ (middle right), excess selectivites (enantiomeric excess, ee, and "branched" excess, be; lower left), and the fitted values (eqs 8−11, solid and dashed lines) versus CO partial pressure at 80 °C, 40 psi H_2 partial pressure, $[Rh]_{TOT} = 6.7 \times 10^{-4}$ M, $[\text{styrene}]_0 = 2.9$ M. All rates measured over the first 10% consumption of styrene.

constant ($k_{exchange}$) the one parameter fit was equivalent to the two parameter fit: the data for $k_{exchange}$ can be described most simply as inverse first-order in P_{CO}. The empirical value of $k_{branched(R)}$ is modeled marginally better with a two parameter fit. Thus, a good fit to all of the data can be obtained with four or five parameters obtained from a sensible kinetic model.

$$k_{linear} = \frac{K_{CO}(K_{Sty(R)}k_{\mathbf{3l(R)}} + K_{Sty(S)}k_{\mathbf{3l(S)}})}{P_{CO}} \approx \frac{2.59}{P_{CO}} \tag{6}$$

$$k_{branched(S)} = \frac{K_{CO}K_{Sty(S)}k_{\mathbf{3b(S)}}}{P_{CO}} \approx \frac{1.70}{P_{CO}} \tag{7}$$

$$k_{branched(R)} = \frac{K_{CO}K_{Sty(R)}k_{\mathbf{3b(R)}}k_{\mathbf{4b(R)}}}{k_{-\mathbf{3b(R)}} + k_{\mathbf{4b(R)}}P_{CO}} \approx \frac{0.27}{1 + 0.0034P_{CO}} \quad \text{(two parameter fit)}$$
$$k_{branched(R)} = \frac{K_{CO}K_{Sty(R)}k_{\mathbf{3b(R)}}k_{\mathbf{4b(R)}}}{k_{-\mathbf{3b(R)}} + k_{\mathbf{4b(R)}}P_{CO}} \approx 0.27 \quad \text{(one parameter fit)} \tag{8}$$

$$k_{\text{exchange}} = \frac{^1/_3 K_{CO} K_{Sty(R)} k_{\mathbf{3b(R)}} k_{-\mathbf{3b(R)}}}{P_{CO}(k_{-\mathbf{3b(R)}} + k_{\mathbf{4b(R)}} P_{CO})}$$
$$\approx \frac{66}{P_{CO}(1 + 0.0P_{CO})} \quad \text{(two parameter fit)}$$
$$k_{\text{exchange}} = \frac{^1/_3 K_{CO} K_{Sty(R)} k_{\mathbf{3b(R)}} k_{-\mathbf{3b(R)}}}{P_{CO}(k_{-\mathbf{3b(R)}} + k_{\mathbf{4b(R)}} P_{CO})}$$
$$\approx \frac{66}{P_{CO}} \quad \text{(one parameter fit)} \tag{9}$$

Although the kinetic data are insufficient to uniquely determine the nine independent rate constants of the model depicted in Scheme 9 and eqs 2−5, with reasonable assumptions these equations do accommodate all the observed rate, selectivity, and exchange data under all conditions. For example, assuming equilibrium constant values for K_{CO}, $K_{Sty(R)}$, and $K_{Sty(S)}$ that are compatible with the observation of rates that are inhibited by CO and first order in styrene, an adequate fit to all of the observed data may be obtained by varying $k_{\mathbf{3l(R)}}$, $k_{\mathbf{3l(S)}}$, $k_{\mathbf{3b(R)}}$, $k_{\mathbf{3b(S)}}$, $k_{\mathbf{4b(R)}}$, and $k_{-\mathbf{3b(R)}}$ (see the Supporting Information for details). Although these rate constants are not uniquely determined, the foregoing demonstrates that the proposed kinetic model accommodates all of the observed data. It must be noted, however, that other, so far unimagined, kinetic scenarios might equally well account for these data.

CO Pressure Effects Originate from Kinetic Competition along the Manifold That Produces 3(R). The proposed kinetic model features reversible formation of the fastest formed rhodium alkyl, **Db(*R*)**, and irreversible formation of rhodium alkyls **Db(*S*)** and **Dl**. The branched:linear and enantiomer ratios are given by eqs 10 and 11. In the limit of very high CO pressure, trapping of **Db(*R*)** becomes faster than the β-hydride elimination ($k_{\mathbf{4b(R)}}[CO] \gg k_{-\mathbf{3b(R)}}$). In this pressure regime, the favored enantiomer and regioisomer are determined by the equilibrium concentration of the diastereomeric alkene bound complexes ($K_{Sty(R)}/K_{Sty(S)}$) and the relative rates at which they undergo hydride addition ($k_{\mathbf{3b(R)}}/k_{\mathbf{3b(S)}}$). The enantiomeric ratio and b:l ratio (see eqs 10 and 11) therefore approach independence with respect to the CO pressure as the pressure is raised.

$$\frac{b}{l} = \frac{\text{rate}^{\mathbf{3(S)}} + \text{rate}^{\mathbf{3(R)}}}{\text{rate}^{\mathbf{2}}} = \frac{K_{Sty(S)} k_{\mathbf{3b(S)}} + \dfrac{P_{CO} K_{Sty(R)} k_{\mathbf{3b(R)}} k_{\mathbf{4b(R)}}}{k_{-\mathbf{3b(R)}} + k_{\mathbf{4b(R)}} P_{CO}}}{K_{Sty(R)} k_{\mathbf{3l(R)}} + K_{Sty(S)} k_{\mathbf{3l(S)}}} \tag{10}$$

$$\frac{\mathbf{3(R)}}{\mathbf{3(S)}} = \frac{\text{rate}^{\mathbf{3(R)}}}{\text{rate}^{\mathbf{3(S)}}} = \frac{\dfrac{P_{CO} K_{Sty(R)} k_{\mathbf{3b(R)}} k_{\mathbf{4b(R)}}}{k_{-\mathbf{3b(R)}} + k_{\mathbf{4b(R)}} P_{CO}}}{K_{Sty(S)} k_{\mathbf{3b(S)}}} =$$
$$k_{\mathbf{4b(R)}} \cdot \frac{k_{\mathbf{3b(R)}}}{k_{\mathbf{3b(S)}}} \cdot \frac{K_{Sty(R)}}{K_{Sty(S)}} \cdot \frac{P_{CO}}{k_{-\mathbf{3b(R)}} + k_{\mathbf{4b(R)}} P_{CO}} \tag{11}$$

In the low CO pressure limit, the branched rhodium alkyl, **Db(*R*)**, undergoes β-hydride elimination faster than it is converted to the corresponding acyl ($k_{\mathbf{4b(R)}}[CO] \ll k_{-\mathbf{3b(R)}}$). The rate of formation of **3(*R*),** is determined by the rate of formation of **Db(*R*)**, which is inversely dependent on P_{CO}, multiplied by a trapping efficiency factor equal to $k_{\mathbf{4b(R)}}P_{CO}/(k_{\mathbf{4b(R)}}P_{CO} + k_{-\mathbf{3b(R)}})$. Under conditions of low pressure the trapping efficiency of **Db(*R*)** increases linearly with increasing CO pressure. In this pressure regime, the inhibitory effect of CO on the rate of formation of **Db(*R*)** cancels the promoting effect on trapping efficiency to yield a net rate of **3(*R*)** formation that is independent of P_{CO}. Because the rate of formation of **3(*S*)** and **2** is inhibited by CO pressure under all observed conditions, the overall enantioselectivity and regioselectivity increase with increasing CO in the low pressure regime.

It is common to identify individual steps in the catalytic cycle as "enantiodetermining", "regiodetermining", or "turnover-limiting". However, such language is too simplistic to encompass the kinetic behavior observed for enantioselective styrene hydroformylation over a broad range of CO pressures. In the limit of high pressure, ratios of product enantiomers and regioisomers are controlled by the relative transition state free energies for insertion of styrene into Rh-H. In this limit, which corresponds to Curtin−Hammett conditions with respect to alkene coordination, one can reasonably speak of insertion as selectivity-determining and turnover-limiting. However, at lower pressures the situation is more complex: intermediates **Dl** and **Db(*S*)** are committed to form **2** and **3(*S*)** but **Db(*R*)** is not. The fate of **Db(*R*)** is controlled by a kinetic competition between transition states (for deinsertion to give **C(*R*)** versus CO association and insertion to give aldehyde product **3(*R*)**) that are similar in free energy.

Enantiofacial Discrimination Largely Controls Regioselectivity. Hydride addition to the *si* enantioface of styrene is nonregioselective, providing a 1:l mixture of branched and linear aldehydes. In contrast, hydride addition to the *re* enantioface of styrene displays excellent regioselectivity (22:1 b:l). Thus, the enantiofacial selectivity of styrene binding strongly impacts both enantioselection and regioselection. This observation suggests that changes in catalyst design that promote discrimination in binding the *re* versus the *si* enantioface of styrene to the catalyst could result in greater regioselectivity and enantioselectivity.

Qualitative Free Energy Surface Depicting the Influence of CO Pressure on Enantioselectivity. The CO pressure strongly influences the hydroformylation selectivities of aryl alkenes such as styrene but not other alkenes. Similarly, deuterioformylation is more likely to result in D exchange into the alkene for aryl alkenes than for other substrates.[18] When styrene does undergo D exchange, it does so primarily at the β-position via the benzylic Rh-alkyls (**Db(*R*)** and **Db(*S*)**). These data suggest the possible involvement of η^3-coordination modes. For example, van Leeuwen[23] has proposed for nonenantioselective hydroformylation of styrene that the initial unsaturation at Rh resulting from alkene insertion into the Rh-H bond is "released by coordination in an η^3-fashion." This coordination mode inhibits CO association, slows conversion to an acyl intermediate, and the "Rh-η^3-1-phenethyl remains in a state that may easily undergo deinsertion." In this model, η^3-coordination decelerates formation of the acyl intermediate. However, our data indicate that alkyl **Db(*R*)** is formed fastest and quasi-reversibly while yielding *most* of the aldehyde product; stabilization of the intermediate **Db(*R*)** by η^3-coordination should *slow* aldehyde production along this path relative to other paths.

An alternative, simpler explanation for the high susceptibility of the alkyl **Db(*R*)** to revert to Rh-H and alkene and for the influence of CO pressure on regio- and enantioselectivitiy is that *the barrier for styrene insertion to give* **Db(*R*)** is uniquely low. This is depicted in the hypothetical free energy surfaces for low and high CO pressure conditions shown in Figure 5.

(23) van Rooy, A.; Orij, E. N.; Kramer, P. C. J.; van Leeuwen, P. W. N. M. *Organometallics* **1995**, *13*, 34–43.

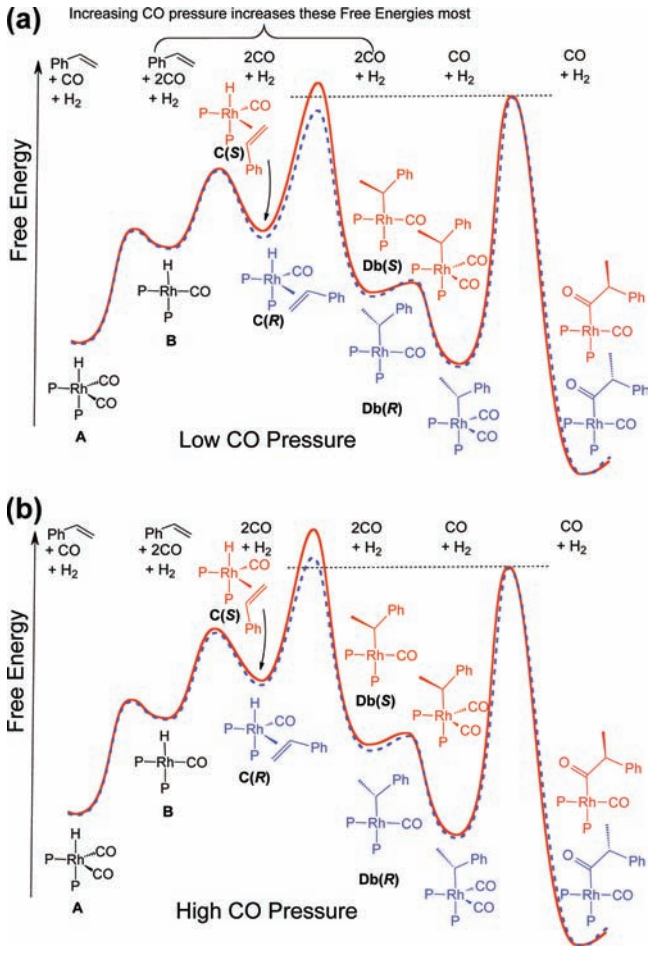

Figure 5. Hypothetical free energy surfaces for low CO pressure (a) and high CO pressure (b) conditions that illustrate the relative increase in rate of *S*-branched aldehyde (red, solid) versus the *R*-branched aldehyde (blue, dashed) with increasing CO pressure. Free energy surfaces for the formation of linear products are not shown explicitly but closely track the *S*-branched (red, solid) surface. This figure provides a graphical depiction of the kinetic behavior only; no additional information such as computed energies are represented.

Free energy surfaces for the formation of linear products are not shown explicitly but closely track the *S*-branched (red, solid) surface. Note that these surfaces do not represent the full catalytic cycle and end at the last kinetically relevant intermediates, acyl complexes. At low CO pressure, the branched alkyl **Db(*R*)** reverts to the styrene adduct because the reversion barrier is lower than the barrier for association of CO and migratory insertion to form an Rh-acyl. Increasing the CO pressure increases the free energy of states having two free CO's to a greater extent than those with one free CO. Thus, at high CO pressure, the barrier of deinsertion becomes higher than association of CO and migratory insertion to form an acyl complex. Under these conditions, insertion of styrene to give the kinetically preferred, branched alkyl **Db(*R*)** becomes irreversible and the observed regioselectivity reached its maximum value. Because the two diastereomeric pathways for making linear aldehydes approximately track the *S*-branched surface, then the increase in enantioselectivity with increasing CO pressure has the same origin as the enantioselectivity increase. Accordingly, if there is a role of η^3-coordination in this model, it is to lower the energy of the transition state that connects **C(*R*)** and **Db(*R*).**

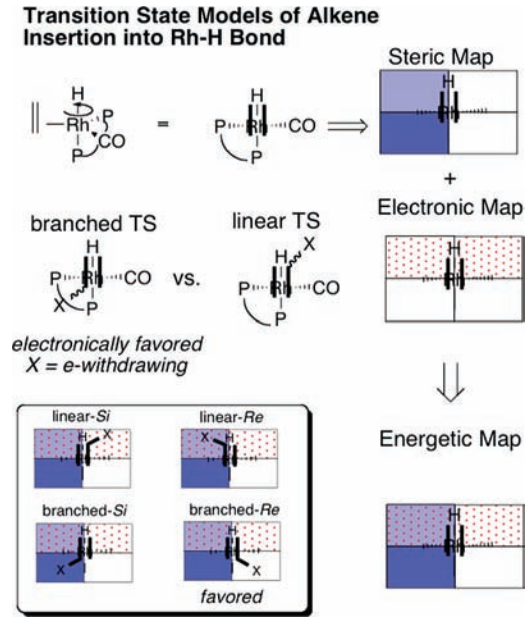

Figure 6. Empirical steric-electronic map that rationalizes observed regioselectivity and enantioselectivity patterns for the hydroformylation of monosubstituted alkenes using Rh(BisDiazaphos) catalysts.

Although the empirical data from this kinetic study are insufficient to determine all of the intermediate and transition state free energies, the surfaces graphically summarize the primary features of the kinetic behavior. Salient features include (1) dissociation of CO from **A** to give **B** is uphill and reversible, (2) styrene binding to **B** at either enantioface is energetically unfavorable with respect to the resting state **A** and rapidly reversible, (3) at low CO pressure, formation of **Db(*S*)** is irreversible which leads to an enantiomeric ratio that is determined by the free energy difference between the transition state for acyl formation on the *S*-branched pathway and the insertion transition state for alkyl formation along the *R*-branched, and (4) at high pressure of CO, conversion of **C(*S*)** to give **Db(*S*)** is irreversible and the enantiomeric ratio is determined by the relative free energies of the styrene insertion transition states, leading to an increase in enantioselectivity.

Qualitative Steric-Electronic Map for Understanding Relative Rates of Insertion of Styrene into Rh-H Bonds. The dominant source of enantioselectivity and regioselectivity in styrene hydroformylation as catalyzed by Rh(BisDiazaphos) complexes is the kinetic preference for styrene insertion to give the branched alkyl **Db(*R*)**. Previous studies by our group have demonstrated a strong Hammett-like correlation for which more electron-withdrawing para subsituents significantly increase the branched:linear ratio but have no systematic effect on the enantiomeric ratio.[6] Substrate electronic factors control, to a first approximation, regioselectivity but not enantioselectivity. Consistent with the trend observed for *para*-substituted styrenes, we generally find that monosubstituted alkenes undergo hydroformylation with higher branched:linear ratios as the inductive effect of the substituent becomes more electron withdrawing (for example, allyl cyanide vs 1-decene). However, the general sense of chiral induction favors addition of the formyl to the *re* face of the alkene for all 1-alkenes examined by us so far. Enantioselectivity is primarily controlled by steric interactions in the diastereomeric transition states for styrene insertion into the Rh-H bond.

Figure 6 depicts a qualitative steric-electronic map that summarizes these findings. We presume that the pseudo-five coordinate transition state structure for alkene insertion favors axial−equatorial coordination of the diphosphine ligand. A two-dimensional quadrant steric map is constructed such that the plane of the map contains the Rh-H vector and lies parallel to the plane of alkene C═C. Because the axial P atom lies in the plane of the map and the equatorial P atom lies behind the plane, the steric influence of the axial P substituents dominates. The equatorial CO ligand is small and exerts minimal steric effect, leading to a quadrant coloring with two sterically small quadrants (uncolored, right-hand side), one quadrant that is sterically large (bottom left, dark blue), and one that lies between the two extremes (top left, light blue). Electronic effects can be superimposed by coloring the top two quadrants (red dots), indicating that orientation of an alkene substituent in the quadrants that give rise to linear products is disfavored. The strength of the electronic effect varies with the inductive effect of the X substituent. As shown in Figure 6, this map rationalizes that the most favored transition state corresponds to the branched-*Re* orientation while the least-favored transition state corresponds to the linear *re* orientation. The free energies of the linear and branched *si* face orientations lie between these extremes.

Are the qualitative ideas presented by Figures 5 and 6 convenient fantasy or an essential representation of the free energy landscape? Insight requires further experimental data and/or computer modeling. On the experimental side, trapping of key intermediates and direct measurements of their relative reactivities would provide critical information. Full computational modeling of the reaction free energy surface, although a daunting task, would enable verification of these hypothetical models.

Summary

Rhodium catalysts bearing the chiral BisDiazaphos ligand exhibit extraordinary rates and regio- and enantioselectivities for the hydroformylation of alkenes. Aryl alkenes, such as styrene, yield branched aldehydes with high enantiomeric purity under optimized conditions, but the regioselectivity and enantioselectivity erode as the syngas pressure is lowered. It is the CO partial pressure, not that of dihydrogen, that influences b:l and enantiomer ratios. Deuterioformylation studies demonstrate that formation of the branched rhodium alkyl that ultimately yields the major enantiomeric aldehyde is reversible, whereas other diastereomeric branched and linear rhodium alkyls are formed irreversibly. Thus, the pressure effect on regio- and enantioselectivity arises from a kinetic competition between CO-dependent conversion of one branched rhodium alkyl diastereomer to an acyl and its reversion to a rhodium hydride and styrene. Studies with deuterium-labeled styrene establish that coordination of *re* versus *si* enantiofaces of styrene leads to very different branched:linear ratios. Models of the reaction free energy surfaces under different CO pressures and steric-electronic mapping of the transition state for insertion of bound styrene into the Rh-H bond provide a graphical summary of the key experimental findings. By exhibiting strong CO pressure effects on regio- and enantioselectivity, aryl alkenes appear to be the exception rather than the rule. It appears that the origin of these effects is the unusually low insertion barrier for formation of a single branched alkyl diastereomer vis-à-vis the free energy of its CO-dependent pathway for acyl formation. These studies constitute a rare example in which the details of regio- and enantioselection can be elucidated for a useful enantioselective hydroformylation catalyst.

Experimental Methods

Tetrahydrofuran (THF) and toluene were distilled over Na/benzophenone and further deoxygenated by at least three freeze−thaw cycles prior to use. $Rh(acac)(CO)_2$ was recrystallized from toluene/hexanes (green needles) prior to use. Dodecane and styrene were purchased from Aldrich, distilled under vacuum, and deoxygenated prior to use. (*R*)-Diphenylprolinol silyl ether was purchased from Aldrich and used as received. α-Deuteriostyrene and nitroethylene were prepared according to literature procedures.[19,24] ^1H NMR and ^2H NMR (76.77 MHz) NMR data were recorded using a Varian Unity 500 MHz spectrometer. Gas chromatography (GC) was performed on a Varian Chrompack instrument using a β-DEX 120 column from Supelco, (30 m × 0.25 mm i.d.). All reaction pressures are reported as absolute pressures in pounds per square inch (psi; **not** gauge pressures, psig).

General Procedure for Asymmetric Hydroformylation. Ligand solutions (THF) and $Rh(acac)(CO)_2$ (toluene) were prepared at room temperature in a nitrogen-filled drybox at room temperature. Hydroformylation solutions were prepared by addition of ligand (1 μmol) and $Rh(acac)(CO)_2$ (0.5 μmol) stock solutions to an oven-dried 50 mL pressure bottle equipped with a magnetic stir bar. Styrene (4.4 mmol) containing dodecane (0.4 mmol) was added, and the total volume was adjusted to 1.5 mL by addition of toluene. The pressure bottle was then connected to a gauged pressure reactor assembly and removed from the drybox. The pressure reactor was then purged three times with syngas (1:1 CO/H_2) and then charged to 150 psi. The reaction bottle was then placed in the oil bath with vigorous stirring and allowed to react for 2 h. After 2 h, the reaction was removed from the oil bath, cooled in an ice bath, and vented.

General Procedure for Deuterioformylation Kinetic Studies. Deuterioformylation solutions were prepared by addition of ligand (1 μmol) and $Rh(acac)(CO)_2$ (0.5 μmol) stock solutions to an oven-dried 50 mL pressure bottle equipped with a magnetic stir bar. The total volume of each reaction was adjusted to 0.9 mL by addition of toluene. The pressure bottle was then connected onto a gauged pressure reactor assembly, and the reactor was removed from the drybox. The reactor was purged three times with CO, charged with 40 psi CO followed by 40 psi D_2, and allowed to stir in an 80 °C oil bath for 30 min. After 30 min, styrene (4.4 mmol) containing dodecane internal standard (0.4 mmol) was added via gastight syringe. Samples for NMR analysis were removed after 5 and 11 min via gastight syringe.

High Pressure IR Spectroscopy. A solution of $Rh(acac)(CO)_2$ (1 μmol), **1**(1.2 μ mol), styrene (5 mmol), and toluene (3.5 mL) was placed in a high-pressure reaction vessel fitted with an in situ attenuated total reflectance IR detector of a ReactIR apparatus. The pressure vessel was sealed under nitrogen and removed from the glovebox. The autoclave was heated to 80 °C followed by pressurization with syngas (1:1 CO/H_2), with rapid stirring. IR spectra were recorded every 2 min. Recording was started 30 s before addition of syngas. The appearance of aldehydes was monitored as the change in intensity of the absorption peak centered at 1725 cm^{-1} corresponding to the overlapping carbonyl stretching frequencies of the branched and linear aldehydes.

Organocatalytic Michael Addition. Organocatalytic Michael reactions were performed in a manner similar to that reported by Gellman and co-workers.[21] To a 12 mL vial equipped with a small magnetic stir bar were added 1.2 mL of dry toluene, (*R*)-diphenylprolinol silyl ether (0.4 mL stock solution in toluene, [catalyst] = 0.05M), 0.2 mmol 3-nitrobenzioc acid B (33.4 mg), and the crude hydroformylation products (approx 2.0 mmol neat).

(24) Wright, J. P.; Gaunt, M. J.; Spencer, J. P. *Chem.−Eur. J.* **2006**, *12*, 949–955. See the Supporting Information for detailed procedures.

The mixture was stirred in an ice bath for 5 min, followed by addition of 1.0 mmol nitroethylene (0.2 mL stock toluene solution). The mixture was stirred in a cold room (3 °C) for 4 days. After 4 days, toluene was removed under reduced pressure, and the product purified via SiO_2 column chromatography eluting with EtOAc (20%) in hexanes to give the (*S*)-2-benzyl-4-nitrobutanal. ^{1}H NMR (500 MHz, C_6D_6): δ 1.46 (m, 1H), 1.70 (m, 1H), 2.08 (X, 1H), 2.15 (dd, $J = 7.5$, 14 Hz, 1H), 2.42 (dd, $J = 7.5$, 14 Hz, 1H), 3.64−3.68 (AB, 2H), 7.0−7.21 (m, 5H),9.0 (s, 1H).

Acknowledgment. This work was supported by the National Science Foundation (CHE-0715491). We thank Professor Charles P. Casey for helpful discussions concerning the mechanistic aspect of this work. Dr. Tulay Atesin performed the molecular mechanics simulation of rotamer populations used in analyzing the enantiofacial origins of enantioselective hydroformylation. NMR instrumentation used in this work was supported by the following grants: NSF CHE-0342998, NIH 1 S10 RR13866-01, NSF CHE-9629688, and NSF CHE-9208463.

Supporting Information Available: Details of NMR and GC analyses of hydroformylation and deuterioformylation products, tabulation of all kinetic and product distribution data (Table S1), phenomenological rate constants and errors determined by fitting observed product distributions to the simple kinetic model of Scheme 6 (Table S2), details of the preparation of α-d_1-styrene and the analysis of linear hydroformylation products derived therefrom, results of fitting rate constants to experimental data according to eqs 6−9, and tabulation of observed data and values calculated from a set of reasonable, assumed kinetic constants. This material is available free of charge via the Internet at http://pubs.acs.org.

JA909619A